

Recrystallization studies in solid-solution alloys of Cu-Ag-Al

O. K. CHOPRA, P. NIESSEN

Department of Mechanical Engineering, University of Waterloo, Waterloo, Ontario, Canada

The isothermal recrystallization kinetics of rolled Cu-Ag alloys containing up to 1.2 at. % Al have been followed metallographically and by hardness measurements and the nucleation rates measured by X-ray back-reflection techniques. Electron-microscopic studies have been carried out to characterize the as-deformed structures and the structural changes occurring during the annealing process. The recrystallization of the alloys was retarded as the aluminium content increased. Nucleation occurred both in the bulk and along the existing grain boundaries and the rates of nucleation varied with time. These effects have been found to be dependent on the deformation structure, alloy composition and the temperature of anneal. The process of grain-boundary migration during recrystallization was very anisotropic and this has been shown to be caused primarily by the nature of the deformation structure.

1. Introduction

Primary recrystallization is generally recognized to involve nucleation and growth of new grains and for the control of recrystallized structures it is desirable to know how these two mechanisms interact and how they depend on the various material and process variables. Unfortunately, direct and independent measurements of nucleation rates and growth rates are extremely difficult. Therefore, much effort has been expended on the analysis of the kinetics of isothermal reversion of deformed metals to their fully annealed state in the hope of obtaining separate values for the nucleation and growth rates.

Generally, isothermal recrystallization kinetics are expressed in terms of the Avrami equation:

$$x = 1 - \exp(-kt^n)$$

where x is the volume fraction recrystallized, t is the annealing time and k and n are constants. The values of n are commonly found to be in the range of 1-3 depending on the influence of alloy composition, mode and amount of deformation and the temperature of anneal on the underlying basic processes. The value of n and its change as a function of various experimental variables has often been used to construct mechanistic recrystallization models. The correct-

ness of such models cannot be directly shown; however, some kinetic experiments indicate that rates of nucleation and growth vary with time [1-4] and show that in solid solution alloys the overall recrystallization process is retarded with increasing solute content [4-8].

In attempts to obtain greater information regarding the mechanism of recrystallization, thin-film electron microscopy has been employed. Several investigations have been carried out in recent years using this technique to study the structural changes occurring during the isothermal anneal of deformed structures [9-12]. These observations support the various models which have been advanced for the mechanism of nucleation [13-15]. However, it seems that no one model is correct for all metal systems over a range of deformation and annealing conditions.

The usefulness of the kinetic results depends on the degree to which the various processes occurring during the recrystallization of deformed metals can be physically realized and incorporated in the phenomenological description. Very few studies have correlated the kinetic and microscopic data for recrystallization. This study is an attempt to study in detail the total recrystallization process of solid-solution alloys combining both the kinetic and microscopic aspects.

2. Experimental procedure

2.1. Alloy preparation

The alloys studied in this investigation were copper containing 0.04 at. % silver and 0.0, 0.1, 0.5 and 1.2 at. % aluminium. The alloys were prepared from oxygen-free high-purity copper and 59 grade aluminium. The silver was added to eliminate the effect of residual impurities.

It is generally known that the presence of low concentrations of residual impurities can strongly influence the recrystallization behaviour of metals. This unpredictable effect of impurities can be eliminated by either refining the metal to very high purities or through the controlled addition of an element to such levels that the residual impurity effect is masked. It has been shown [7] that the addition of only 0.015 at. % silver increases the recrystallization temperature of copper and eliminates the influence of the common impurities in copper.

Each alloy was prepared by melting appropriate proportions of OFHP copper and a master-alloy containing 5.0 wt. % aluminium in an induction furnace using a graphite crucible. The melt was covered with charcoal powder to avoid oxygen contamination and was bottom poured into a split graphite mould of 6.5×0.6 cm cross section. The as-cast bars were machined and cold-rolled to 3.5 mm thickness. Specimens of 12×12 mm size were cut from the rolled strip and annealed at 800°C for 24 h under an argon atmosphere and furnace cooled to room temperature. The final grain size of the alloys was between 0.2 to 0.6 mm.

2.2. Recrystallization experiments

The specimens were given a final 50% reduction by rolling at room temperature. Annealing of the deformed specimens was carried out in a binary nitrate salt bath. The temperature of the bath was controlled to within $\pm 1^\circ\text{C}$. The recrystallization process was studied by conducting isothermal recrystallization experiments and measuring the fraction recrystallized and nucleation rate, and by structural observations using optical and transmission electron microscopy.

The recrystallized fraction after different annealing times was followed by metallographic and hardness measurements. A two-dimensional systematic point count method described by Hilliard and Cahn [16] was used for quantitative metallographic measurements. The hardness

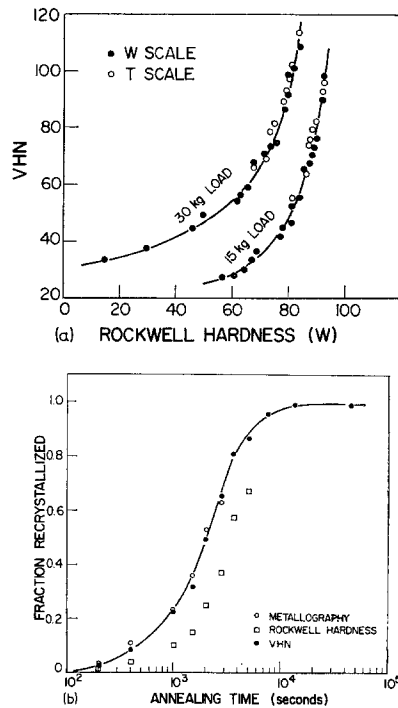


Figure 1 (a) Relationship between Rockwell W hardness and the Vickers hardness (b) Comparison between the values of fraction recrystallized measured by metallography and those determined from the decrease in Rockwell and Vickers hardness.

measurements were performed on a Rockwell Superficial Hardness Tester using the Rockwell W scale. These hardness numbers were converted to Vickers Hardness numbers using the correlation curve shown in Fig. 1a. The values of fraction recrystallized were obtained from the decrease in VHN as a function of time. A comparison between the measured values of fraction recrystallized and those obtained from the decrease in VHN is shown in Fig. 1b. It can be seen that the values of fraction recrystallized obtained from the two techniques show a very good agreement. Consequently, it was decided to follow the recrystallization behaviour by hardness measurements alone.

The nucleation rate was obtained experimentally by measuring the number of grains appearing as a function of time. This was achieved by taking X-ray back reflection patterns from the specimens which were annealed isothermally for different times after deformation. The back-reflection patterns were in the form of Debye rings. The number of discrete reflections on a particular ring is proportional to the number

of grains appearing during the recrystallization process. The specimens were traversed back and forth over 1 cm to gather reflections from a large area of the specimen. For each specimen several portions on the sample surface were traversed to obtain a meaningful average value for the number of grains.

The structure of the deformed and the annealed specimens at various stages of recrystallization was examined by transmission electron microscopy. Foils were prepared from the bulk material by mechanical and chemical thinning. The final thinning was carried out by jet-polishing using an electrolyte of 30% orthophosphoric acid.

3. Experimental results

3.1. Recrystallization kinetics

The recrystallization curves as a function of the decrease in hardness after isothermal annealing at different temperatures for various annealing times were obtained for all the alloys. A typical example of these softening curves is given in Fig. 2a. In all cases the marked hardness decrease coincided with the recrystallization process observed metallographically and the decrease in VHN corresponded to the volume fraction recrystallized.

These results indicate that for a given temperature an increase in the aluminium content of the alloy increases the time for the start of recrystallization and decreases the rate of recrystallization. It is not possible to assess the recrystallization start and finish time with any accuracy from the hardness data, due to the relative insensitivity of the measurements for very low and high values of fraction recrystallized. However, the time for 50% decrease in hardness, (i.e. 50% recrystallized) was determined for each alloy and is given in Table I.

In order to verify whether the kinetics of recrystallization follow the Avrami equation, plots of $\ln \ln \{1/(1-x)\}$ versus $\ln t$ were produced and an example is shown in Fig. 2b. The straight lines resulting from these plots show that the recrystallization data do in fact obey this expression. The slope of these plots yields the values of the time exponent n and these are listed in Table I. It can be observed that the values of n are dependent on both the annealing temperature and the aluminium content of the alloy. In general they increase with temperature and decrease with increasing additions of aluminium. Also a deviation from the linear

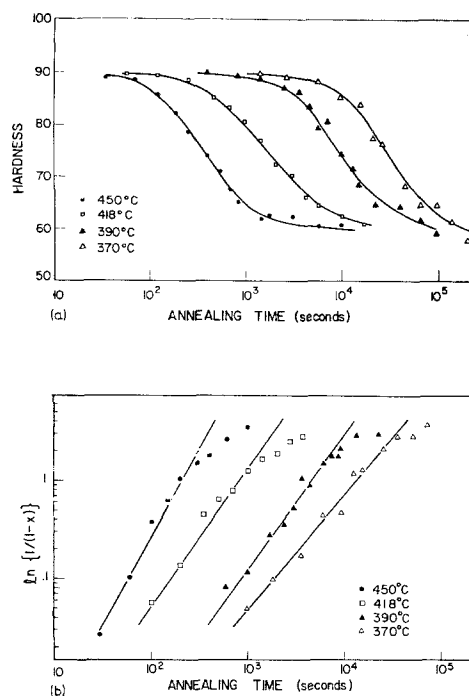


Figure 2 (a) Isothermal recrystallization curves of hardness versus annealing time for Cu-0.04 at. % Ag-1.2 at. % Al alloy after 50% rolling. (b) Plot of the values of the fraction recrystallized " x " with time, obtained from data in Fig. 2a.

relationship is observed for higher values of fraction recrystallized. This deviation starts at lower values of fraction recrystallized for higher annealing temperatures.

Considering the temperature dependence of recrystallization, it is possible to obtain an activation energy for the overall recrystallization process. The rate of recrystallization can be expressed in an Arrhenius form given by:

$$\text{recrystallization rate} = A \exp(-Q/RT)$$

$$\text{or} \quad (1/t) = A' \exp(-Q/RT)$$

where t is the time for a given amount of fraction recrystallized, Q the activation energy, R the gas constant, T the absolute temperature and A' a constant. The activation energy for the process can then be obtained from the slope of the plots of $\ln 1/t$ versus $1/T$. The values of the activation energy obtained from such plots are also given in Table I.

3.2. Nucleation rates

The number of nuclei formed during recrystallization were determined by counting the number of reflections on the Debye rings obtained

TABLE I Kinetics of recrystallization

Aluminium concentration (at. %)	Temperature of anneal (°C)	Time for 50% recrystallization (sec)	Time exponent (<i>n</i>)	Activation energy (kcal/mol)
0.0	360	2100	1.46	
0.1	330	26500	1.86	45.9
	350	7000	1.98	
	370	1800	1.42	
	395	540	1.69	
	430	115	2.60	
0.5	360	16000	1.54	48.3
	380	4400	1.56	
	400	1400	2.17	
	425	380	2.09	
	445	180	2.18	
1.2	370	10000	1.21	48.9
	390	3400	1.48	
	418	580	1.51	
	450	165	1.83	

by X-ray back reflection from a fixed area of the specimen surface. The curves for the number of reflections as a function of time are shown as continuous lines in Fig. 3 for all the alloys. The slope of these curves at various times represent the instantaneous nucleation rate per unit volume of the specimen. It should be noted that as recrystallization proceeds the volume available for the nuclei to form, i.e. the unrecrystallized volume, decreases. The true nucleation rates or the rates of nucleation in the unrecrystallized volume, were obtained from the measured nucleation rates and the overall recrystallization kinetic curves. They are shown as dotted lines in Fig. 3.

It can be seen from these curves that the nucleation rates are not constant but change with time, depending on the alloy composition and temperature of anneal. In general, for a particular alloy the nucleation rates increase with temperature, and for a given temperature they decrease with an increase in the aluminium content of the alloy. Comparison of these curves with the isothermal recrystallization curves shows that nucleation occurs throughout the recrystallization process except in the case of Cu-Ag where the rates decrease to a very low value after 60% of the volume has recrystallized.

3.3. Deformation structure

The structure observed in the as-rolled speci-

mens of Cu-Ag-0.1% Al is characterized by cells whose walls consist of dense dislocation tangles. The typical structure observed in this alloy after 30 and 70% rolling, is shown in Figs. 4a and b respectively. The cells are well developed after 30% rolling. With increasing deformation the cell walls become denser while the cell size remains the same. There is no apparent coalescing or rearrangement of dislocations within the cell walls to form sharp and distinct sub-boundaries. The cell size is observed to vary from 0.5 to 1 μ m.

In contrast to the structure observed in this alloy, the as-rolled specimens of Cu-Ag-1.2% Al alloy does not show a regular cell structure. The structure is characterized by bands of high dislocation density and the regions separating them also show many dislocation tangles. The bands become narrower and the spacing between them decreases with increasing amount of deformation. They are observed to lie parallel to the [110] directions in the foil and are approximately perpendicular to the rolling direction. Figs. 5a and b show structures representative of this alloy after 30 and 70% rolling respectively. It can be seen that there is no apparent coalescing of dislocations into regular cells. In many regions the foil is observed to be practically opaque owing to a dense and uniform distribution of dislocations.

These observations on the character of the

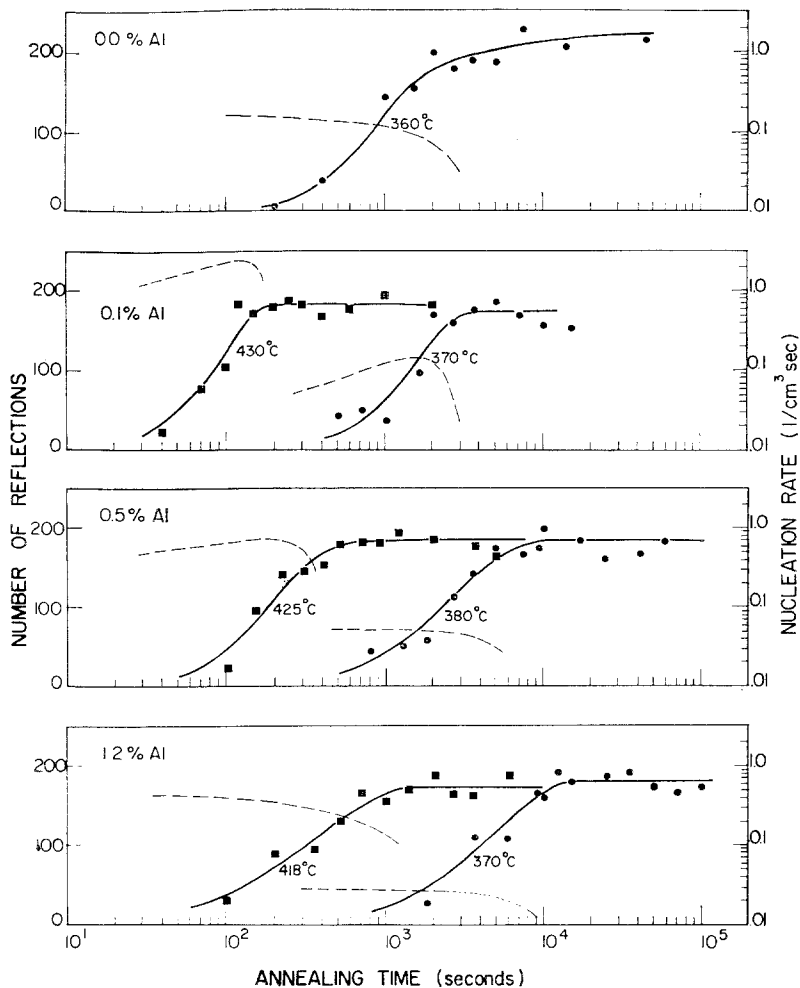


Figure 3 Number of reflections and instantaneous nucleation rates versus annealing time from isothermally annealed specimens of Cu-0.4 at. % Ag-AI alloys rolled 50%.

sub-structure produced after deformation of both these alloys are consistent with the diffraction patterns obtained using the technique of selected area electron diffraction (SAD). The patterns show streaking of the diffraction spots, indicating small but gradual changes in orientation across the structure.

3.4. Structural changes

The microstructural changes which occur during the early stages of annealing show the gradual recovery of the deformation structure to produce embryos or nuclei of strain free grains. The structures observed in the specimens depended upon the time and temperature of annealing. In all cases, nuclei, i.e. new grains bounded by high-angle boundaries separating

the recrystallized and the deformed regions, were observed only after a certain time or incubation period. The appearance of these nuclei coincided with a marked hardness decrease of the specimens. The incubation period was characterized by rearrangement and modification of the deformed structure. The SAD patterns were consistent with these observations and showed the breaking-up of individual reflections into distinct sub-spots indicating the presence of regions with sharp orientation differences. However, a difference in the nature and ease of this formation of nuclei was observed among the different alloys. This difference apparently arises from the variation in the deformation structure of these alloys. In the Cu-Ag-0.1 Al alloy the cell walls become

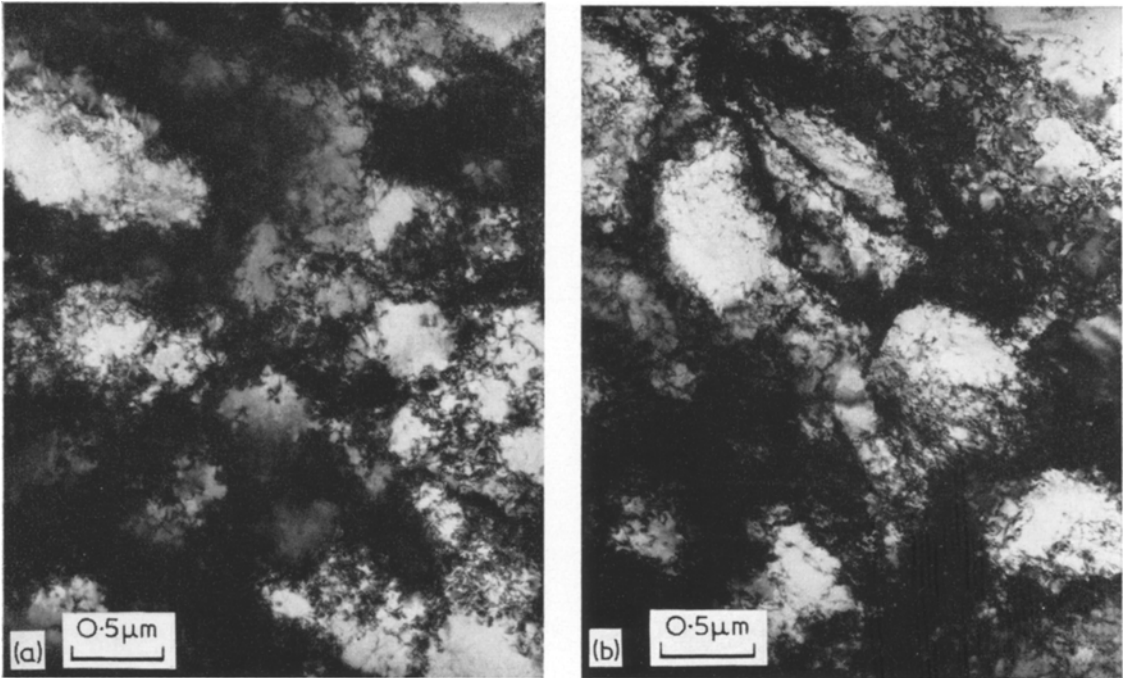


Figure 4 Microstructures after cold rolling of Cu-0.04 at.% Ag-0.1 at.% Al alloy. (a) Rolled 30%; (b) rolled 70%.

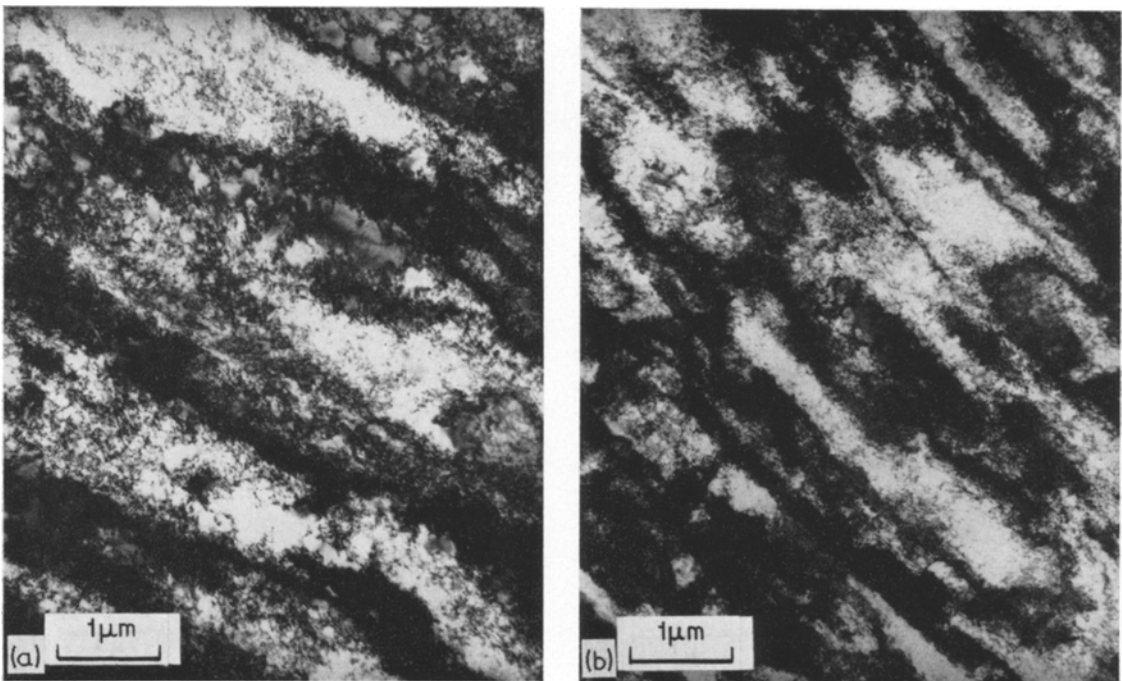


Figure 5 Microstructures after cold rolling of Cu-0.04 at.% Ag-1.2 at.% Al alloy. (a) Rolled 30%; (b) rolled 70%.

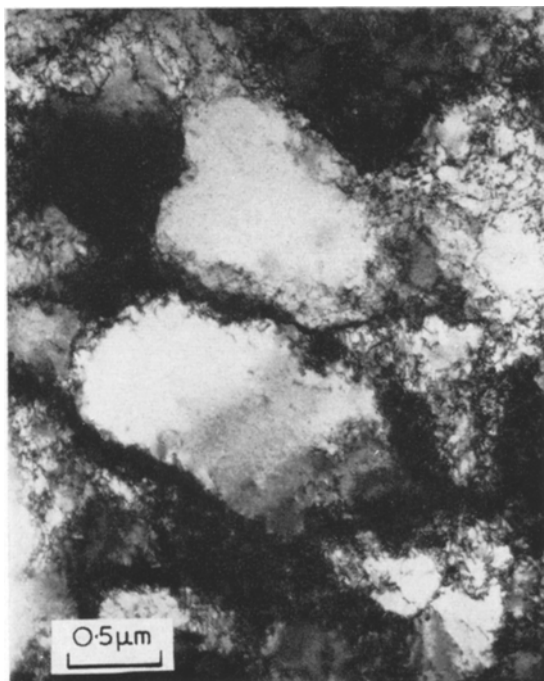


Figure 6 Cu-0.04 at. % Ag-0.1 at. % Al annealed for 150 sec at 395°C after 50% rolling.

sharper by coalescence and rearrangement of dislocations within the cell walls, (Fig. 6); while in the alloy containing 1.2% Al, strain-free regions are formed in the heavily deformed structure requiring disentanglement and motion of dislocations (Fig. 7).

In addition, observations in other regions of the annealed specimens of these alloys show nucleation of new grains via migration of local segments of the pre-existing grain boundary, (Fig. 8). Such a migration process produces bulges in the boundary, and the regions through which it has moved show comparatively few dislocations. The microstructure suggests that the segments of the boundary capable of migrating have a difference in dislocation density across them. The bulging of boundaries into the deformed matrix did not in all cases lead to a complete elimination of the defect structure. In cases where some dislocations are ending in the boundary on the concave side of the bulge, movement of the boundary leads to the extension of these dislocations over the distance of boundary movement, as seen between regions A and B in Fig. 8.

During the later stages of recrystallization

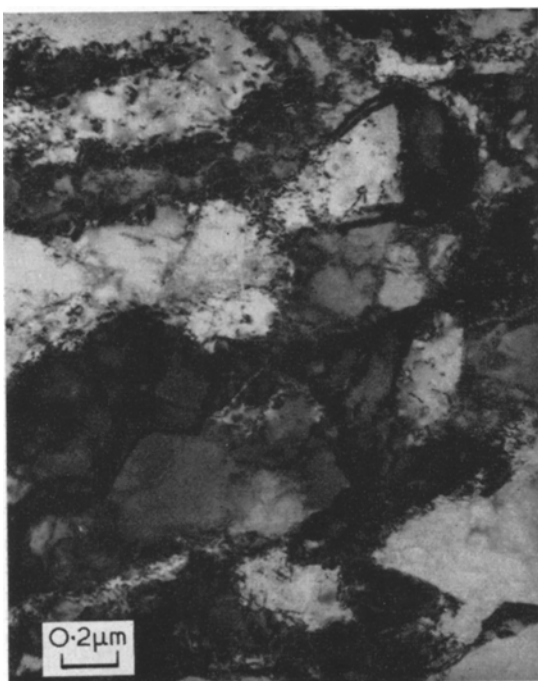


Figure 7 Cu-0.04 at. % Ag-1.2 at. % Al annealed for 30 sec at 450°C after 50% rolling.



Figure 8 Cu-0.04 at. % Ag-1.2 at. % Al annealed for 60 sec at 450°C after 50% rolling.

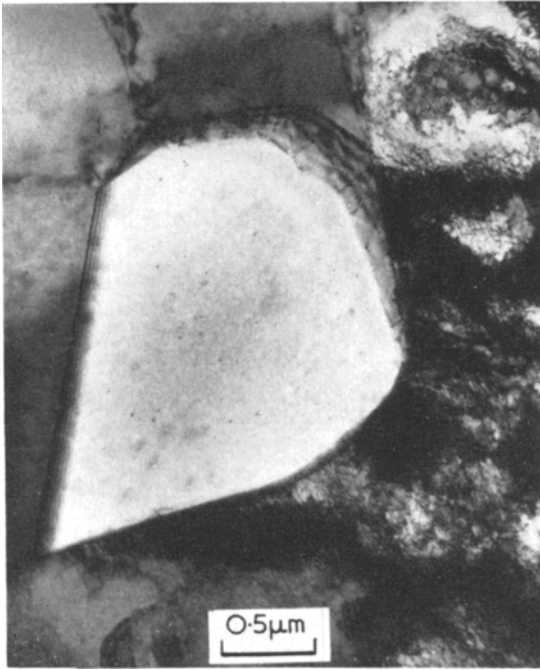


Figure 9 Cu-0.04 at. % Ag-0.1 at. % Al annealed for 2500 sec at 350°C after 50% rolling.

the nuclei of strain-free grains become viable by acquiring a high-angle mobile boundary and grow at the expense of the strained matrix, (Fig. 9). Annealing twins can be seen even during the early stages of growth. The process of grain-boundary migration is observed to be heterogeneous and depends on the deformation structure ahead of the migrating boundary. This can be seen clearly in Fig. 10. The boundary of the growing grain is seen to contain many steps with segments of the boundary migrating along the bands of dislocation tangles.

The optical micrographs are consistent with these observations. Recrystallized grains are observed to form simultaneously along the existing grain boundaries and in the bulk, (Fig. 11). Annealing twins are seen in abundance during the early stages of recrystallization. A typical structure observed after complete recrystallization of these alloys is shown in Fig. 12. It should be noted that the number of twins observed in this structure is considerably less than that observed during the early stages of recrystallization.

4. Discussion

4.1. Recrystallization kinetics

The isothermal recrystallization curves are of a

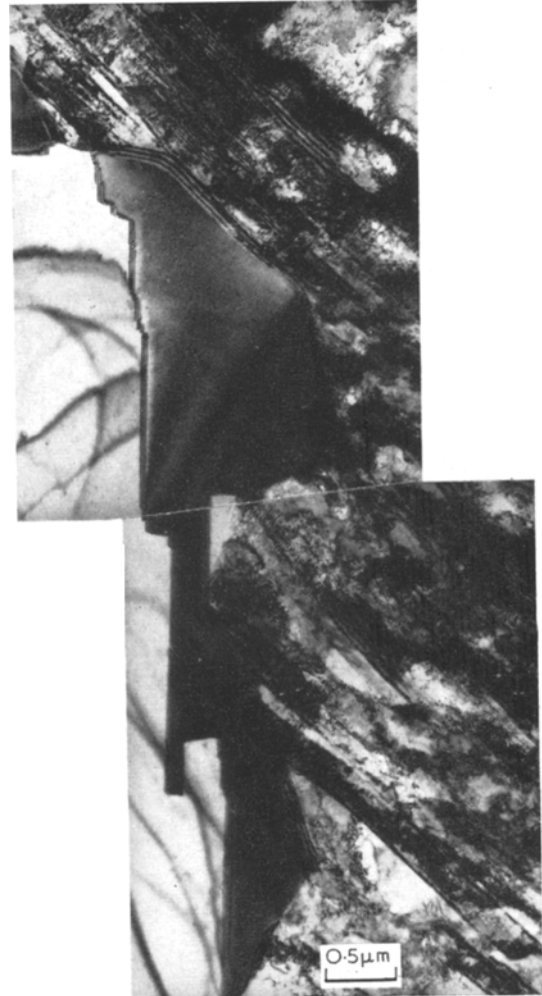


Figure 10 Cu-0.04 at. % Ag-1.2 at. % Al annealed for 1000 sec at 390°C after 50% rolling.

sigmoidal form, characteristic of a nucleation and growth process and can be expressed in the form of the general Avrami equation. The temperature dependence of recrystallization yields a value for the apparent activation energy of the overall recrystallization process. These values suggest that volume diffusion is involved in the process of recrystallization. However, on the basis of this activation energy it cannot be decided whether nucleation or growth is rate controlling. The recrystallization results show that with increasing aluminium content of the alloy, recrystallization is retarded and the overall rates of recrystallization are decreased. The latter is reflected in the change in the values of the time exponent n . The values are

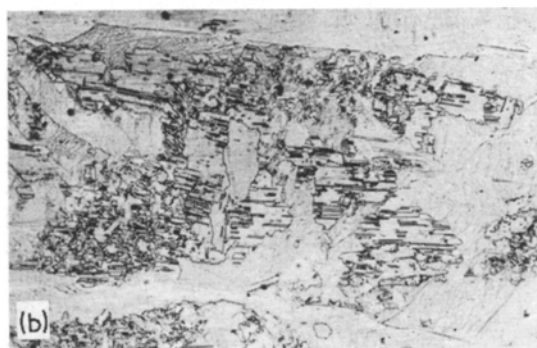


Figure 11 (a) and (b) Cu-0.04 at.% Ag-0.1 at.% Al annealed for 500 sec at 370°C after 50% rolling ($\times 48$).



Figure 12 Completely recrystallized structure in Cu-0.04 at.% Ag-0.1 at.% Al alloy ($\times 80$).

in the range of 1 to 2.5, the exact value being dependent on the alloy composition and the annealing temperature.

A low value of n is considered to imply one- or two-dimensional growth during recrystallization. The effect of solute addition and annealing temperature is generally attributed to the decrease in the driving force for grain-boundary migration due to competing recovery processes

[4, 5]. Recrystallization is retarded to a greater extent for a higher solute content and lower annealing temperatures because both these factors have different effects on recovery and recrystallization. However, such arguments assume that the recrystallization kinetics are basically controlled by the growth rates and that nucleation rates are either constant or that nuclei form at zero time. In the present work it was shown that nucleation starts after an incubation period and occurs throughout the recrystallization process. The rates of nucleation vary with time. This variation depends on the alloy composition and temperature of anneal. In general, the rates are maximum during the very early stages of recrystallization and gradually decrease. Comparing the nucleation rates for different alloys (Fig. 3), it is observed that with increasing aluminium content, the nucleation rates decrease and their variation with time is smaller.

These results suggest that the overall recrystallization behaviour is controlled by both the rates of nucleation and growth. In order to interpret the recrystallization behaviour of these alloys, it will be worthwhile to look at the individual mechanisms of recrystallization.

4.2. Mechanism of recrystallization

The mechanism of recrystallization will be considered in two steps – the first step involving the formation of nuclei which are bounded by high-angle mobile boundaries, and the second, the growth of these nuclei by boundary migration to eliminate the deformation structure.

4.2.1. Nucleation

Electron microscopic observations indicate that nucleation occurs only after an incubation period. The appearance of nuclei is concurrent with a marked decrease in hardness of the samples and the appearance of reflections on the X-ray back-reflection patterns. The micrographs of the structure observed during the early stages of recrystallization show that nuclei form both along the original boundaries by a bulge nucleation model [15] and in the regions of high dislocation density by the Cahn-Cottrell mechanism [13, 14]. The contribution of these mechanisms to the nucleation phenomenon can be understood by considering the microscopic observations and the results of nucleation and recrystallization kinetics.

The bulge nucleation mechanism is essentially

a process of grain-boundary migration and strictly speaking is not a nucleation process. The existing grains advance into its neighbour and acquire a more perfect lattice in the process. The driving force is derived from the differences in dislocation density across the boundary. For this process, the incubation period would be representative of the time during which the growing regions attain a size detectable by our X-ray technique. Consequently, the incubation period will change with temperature due to the temperature-dependence of grain-boundary migration. However, for a given temperature, increasing solute contents should not influence nucleation to a great extent. The alloys used in this investigation contain an appreciable amount of solute and the interaction of the solute with the moving boundary will probably not change greatly over the total range of solute additions. This is particularly true for boundary migration during primary recrystallization, i.e. when the driving force is very high [17]. Yet the kinetic results show a strong influence of solute on the nucleation process. This would suggest that the nucleation phenomenon, in these alloys, is not controlled by the bulge nucleation mechanism but rather that nucleation in the bulk is predominant. This reasoning is also borne out by the relatively small number of bulge nucleation events observed in the course of the electron-microscopic studies.

The bulk nucleation mechanism involves the formation of strain-free grains by the gradual healing of heavily distorted regions in the cold-worked matrix. The effectiveness of this process will depend on the number of highly distorted regions in the matrix and the ease with which a viable strain-free grain can be formed. This latter process requires considerable rearrangement and motion of dislocations and will be strongly temperature dependent. Also, both these processes will depend on the nature of the deformation structure. Increasing amount of solute content will have two separate effects on this nucleation mechanism. First, as was shown, there is a change in the deformation structure, and secondly, the formation and growth of nuclei will be restricted by the more tangled dislocations observed with higher solute content and probably solute adsorption to dislocations will also prevent their efficient rearrangement. Consequently, both solute content and temperature of anneal will effect the nucleation process, the incubation period will increase

with an increase in solute and decrease with annealing temperature, as is seen in the kinetic results.

4.2.2. Growth

In all cases the growth of nuclei occurs by the migration of high-angle boundaries in order to eliminate the defect structure. A very anisotropic behaviour of boundary migration was observed in these alloys. The electron microscopic observations indicate that this obviously arises from the anisotropic nature of the structure produced after deformation. As seen in Fig. 10, the boundary does not move uniformly into the defect structure. The structure ahead of the migrating boundary is inhomogeneous and is composed of bands of dense dislocation tangles. The boundary configuration with respect to the defect structure suggests that the boundary has difficulty moving in the direction perpendicular to the deformation bands. This indicates an apparent dependence of the boundary migration on the type of the dislocation structure encountered by the boundary. It would appear that the anisotropic movement of the boundary is caused not only by the driving force anisotropy but also by the ease with which the boundary can absorb the dislocation structure. The controlling factor for the latter will be the ease of rearrangement of the dislocation structure ahead of the migrating boundary such that it is acceptable to the boundary. In the case of higher annealing temperature or alloys having lower solute contents, the defect structure will be less stable and such recovery processes will be relatively easy.

It is apparent, therefore, that this dependence of the boundary migration on the defect structure would lead to an anisotropic movement of the boundary and control the rates of boundary migration and consequently the overall growth rates. This is reflected in the values of the time exponent n obtained from the isothermal recrystallization kinetics. The values of n are generally low and increase with increasing annealing temperature and decrease with increasing solute content. This cannot be explained on the basis of a change in the nucleation rates alone. In the case of constant and isotropic growth, the values of n should be between 3 and 4 for decreasing nucleation rates [18]. The observed values of n and the deviation of the data points from the linearity of the Avrami plot are consistent with the anisotropic growth

process and its dependence on the alloy composition and annealing temperature.

In this connection it is interesting to note the extremely high twinning frequency observed in these alloys. The large number of annealing twins are believed to be produced in order for the boundary to maintain a high mobility [19, 20]. In general, it was observed that the twins lie perpendicular to the direction of high growth rate and the grains took up a more two-dimensional shape, (Fig. 11b). In this way the migrating boundary splits up in discrete sections between twins so as to maintain high mobility of individual segments. However, this mechanism will become increasingly difficult when the grains have grown to large sizes. The overall rates of boundary migration will consequently decrease.

These arguments indicate that the process of grain boundary migration during primary recrystallization cannot be considered in terms of a "structureless membrane" expanding uniformly into a structureless matrix. The mechanism of boundary migration depends strongly on the deformation structure, and therefore in an interpretation of the kinetics of recrystallization the variation in the nucleation and growth processes cannot be ignored.

5. Conclusions

The isothermal recrystallization behaviour of Cu-Ag-Al alloys has been shown to be a function of the deformation structure, solute content and the temperature of anneal. The overall recrystallization kinetics can be expressed in terms of the Avrami equation and are controlled by both the nucleation and the growth processes.

Nucleation occurs predominantly in the bulk by the gradual healing of the heavily distorted regions and only to some extent along the existing grain boundaries by bulging of the boundary. There is an incubation period before viable nuclei can be formed and this time is controlled by the nature of the defect structure. The rates of nucleation change with time depending on the alloy composition and annealing temperature.

The process of grain-boundary migration during primary recrystallization shows a very anisotropic behaviour. This is believed to be caused by the driving force anisotropy, but particularly by the ease with which the boundary can accommodate the dislocation structure it encounters. The formation of annealing twins seems to play a large role in maintaining high grain-boundary mobilities.

References

1. W. A. ANDERSON and P. F. MEHL, *Trans. AIME* **203** (1955) 1053.
2. E. C. W. PERRYMAN, *Trans. Met. Soc. AIME* **161** (1945) 140.
3. W. C. LESLIE, F. J. PLECITY, and J. T. MICHALAK, *ibid* **221** (1961) 691.
4. R. A. VANDERMEER and P. GORDON; "Recovery and Recrystallization of Metals", edited by L. Himmel (Interscience, New York, 1963) p. 211.
5. L. M. CLAREBROUGH, M. E. HARGREAVES, and M. H. LORETTO, *ibid*, p. 63.
6. V. G. MASING, K. LÜCKE, and P. NOLTING, *Z. Metall.* **47** (1956) 64.
7. W. DAHL and J. GEISSLER, *ibid* **51** (1960) 421.
8. K. T. AUST and J. W. RUTTER, *Trans. Met. Soc. AIME*, **218** (1960) 682.
9. J. E. BAILEY and P. B. HIRSCH, *Phil. Mag.* **5** (1960) 485.
10. W. J. BOLLMAN, *J. Inst. Metals* **87** (1959) 439.
11. J. E. BAILEY and P. B. HIRSCH, *Proc. Roy. Soc. (London)* **A267** (1962) 11.
12. H. HU, *Trans. Met. Soc. AIME* **224** (1962) 75.
13. R. W. CAHN, *Proc. Phys. Soc.* **A63** (1950) 323.
14. A. H. COTTRELL, "Dislocations and Plastic Flow in Crystals" (Clarendon Press, Oxford, 1953) p. 194.
15. J. E. BAILEY, *Phil. Mag.* **5** (1960) 833.
16. J. E. HILLIARD and J. W. CAHN, *Trans. Met. Soc. AIME* **221** (1961) 344.
17. P. GORDON and R. A. VANDERMEER, "Recrystallization, Grain Growth and Textures" (ASM, 1965) p. 205.
18. J. W. CHRISTIAN, "Physical Metallurgy", edited R. W. Cahn (North-Holland, Amsterdam, 1970), p. 471.
19. K. T. AUST and J. W. RUTTER, *Trans. Met. Soc. AIME* **221** (1961) 758.
20. *Idem*, *ibid* **224** (1962) 111.

Received 8 May and accepted 19 June 1972.